Effects of the information-driven awareness on epidemic spreading on multiplex networks

Jun Wang, Weijie Xiong, ⓘD Ruijie Wang, et al.

View Online   Export Citation   CrossMark

Effects of the information-driven awareness on epidemic spreading on multiplex networks

Jun Wang,[1] Weijie Xiong,[2] Ruijie Wang,[3,a] [ID] Shimin Cai,[1] [ID] Die Wu,[4] Wei Wang,[5] [ID] and Xiaolong Chen[6] [ID]

AFFILIATIONS

[1] School of Computer Science and Engineering, University of Electronic Science and Technology of China, Chengdu 611731, China
[2] School of Information and Communication Engineering, University of Electronic Science and Technology of China, Chengdu 611731, China
[3] School of Mathematics, Aba Teachers University, Aba 623002, China
[4] School of Computer Science, Sichuan Normal University, Chengdu 610101, China
[5] School of Public Health and Management, Chongqing Medical University, Chongqing 400016, China
[6] School of Computing and Artificial Intelligence, Southwestern University of Finance and Economics, Chengdu 611130, China

[a] Author to whom correspondence should be addressed: ruijiewang001@163.com

ABSTRACT

In this study, we examine the impact of information-driven awareness on the spread of an epidemic from the perspective of resource allocation by comprehensively considering a series of realistic scenarios. A coupled awareness-resource-epidemic model on top of multiplex networks is proposed, and a Microscopic Markov Chain Approach is adopted to study the complex interplay among the processes. Through theoretical analysis, the infection density of the epidemic is predicted precisely, and an approximate epidemic threshold is derived. Combining both numerical calculations and extensive Monte Carlo simulations, the following conclusions are obtained. First, during a pandemic, the more active the resource support between individuals, the more effectively the disease can be controlled; that is, there is a smaller infection density and a larger epidemic threshold. Second, the disease can be better suppressed when individuals with small degrees are preferentially protected. In addition, there is a critical parameter of contact preference at which the effectiveness of disease control is the worst. Third, the inter-layer degree correlation has a "double-edged sword" effect on spreading dynamics. In other words, when there is a relatively lower infection rate, the epidemic threshold can be raised by increasing the positive correlation. By contrast, the infection density can be reduced by increasing the negative correlation. Finally, the infection density decreases when raising the relative weight of the global information, which indicates that global information about the epidemic state is more efficient for disease control than local information.

Published under an exclusive license by AIP Publishing. https://doi.org/10.1063/5.0092031

The suppression of an epidemic is inseparable from the effective deployment of both public and personal resources, which has long been a vital epidemiological problem. In particular, the deployment of personal resources is influenced by the information-driven awareness of individuals and is adjusted dynamically with the spread of the epidemic. In turn, efficient deployment of personal resources can affect the dynamic characteristics of an epidemic. A systematic study of the interaction between the processes of awareness, resource allocation, and epidemic spreading will be of prime significance in the containment of the epidemic. Here, by considering a series of realistic factors, such as the preferential contact among individuals, the different types of information, and the structure of the underlying networks, we systematically study the impact of awareness that is stimulated by epidemic-related information on the spread of the epidemic. Through both theoretical analysis and Monte Carlo simulations, we find that during a pandemic, resource support among individuals should be more active to suppress the spread of the epidemic. In addition, an epidemic can be suppressed more efficiently when nodes with small degrees are preferentially protected. Moreover, we find that the inter-layer degree correlation has a "double-edged sword" effect on the spreading dynamics. In other words, when there is a relatively lower infection rate, the epidemic threshold can be raised by increasing the positive correlation. By contrast, the infection density can be reduced by increasing the negative correlation. Finally, we find that the infection density decreases when raising the relative weight of the global information, which indicates that global information about the epidemic state is more efficient for disease control than local information.

I. INTRODUCTION

The ultimate goals of studying epidemic dynamics on complex networks are the prevention and control of diseases, and adequate resources are a prerequisite to achieve these goals. However, resources, such as medicines, vaccines, and medical facilities, are often insufficient to meet the treatment and immunization needs of large numbers of infected cases and vulnerable populations induced by the rapid outbreak of an infectious disease.[1,2] For example, as of 15 March 2022, the ongoing coronavirus disease 2019 pandemic propagated at a breakneck speed, leading to the infection of more than 460 million people as well as over 6 million deaths.[3] The surge in the confirmed cases poses a major challenge to the public health system, inducing a critical shortage of medical and protective resources as well as a devastating socio-economic impact on countries around the world,[4–6] which leads to a decline in overall recovery rates and an increase in mortality as it prevents the infected people from obtaining timely testing and treatment.[7] Moreover, the shortage of protective supplies, such as face masks and disinfectants, increases the probability of exposure of susceptible individuals to the virus, which leads to a higher infection probability and consequently accelerates the propagation of the virus.[8]

Extensive practices have demonstrated that both public intervention measures, including international and domestic travel restrictions, closing schools, and strictly limited public gatherings, adopted by many countries, and personal protective measures, such as social distancing, self-isolation, and hand washing, can significantly mitigate the burden of infection.[9,10] However, more important, is the efficient use of limited resources to improve recovery rates and reduce mortality and infection rates. Consequently, efficient allocation of scarce resources plays a vital role in the containment and mitigation of virus propagation during the pandemic. Many scholars have conducted in-depth research from different perspectives using both theoretical modeling and mathematical analysis combined with extensive experimental simulation methods.[11,12] For example, by proposing a convex framework, the authors of Refs. 13 and 14 solved the problem of determining a cost-optimal allocation of resources. Chen *et al.*[15] studied the problem of optimal deployment of limited resources to minimize the prevalence of the disease. Using both the quenched mean-field theory and heterogeneous mean-field approaches, they found that the problem can be solved based on the condition that the cure rate of the node is positively correlated with the medical resource. The above representatives consider the optimal problem statically. Another line of work consider that an efficient strategy of resource allocation should incorporate the dynamic characteristics of the spread of the epidemic.[15–17] A typical example is the research conducted by the authors of Ref. 16. Based on a scalable dynamic message-passing method, the authors proposed a universal framework to address these problems.

Although a large body of literature has addressed the optimal problem under certain conditions, a more efficient strategy of resource deployment should encompass more than the structure of underlying networks and spreading dynamics based on a simple epidemic model. In a more realistic scenario, an epidemic evolves dynamically with the diffusion of information. Specifically, disease transmission stimulates the diffusion of information through various channels, which induces the awareness of susceptible

individuals and alters their behaviors, such as maintaining social distancing and wearing face masks.[18] Changes in individual behavior can, in turn, influence the spreading dynamics of the epidemic by affecting the effective infection rate of the disease or the susceptibility of individuals.[19–22] Consequently, it is essential to systematically understand the interaction mechanisms between awareness and epidemic spread in designing more realistic and efficient strategies for resource allocation.[23–26] The literature Ref. 27 has made the seminal work on studying the coevolution of awareness and disease on networks, and the authors found that the spread of the disease can be suppressed by the diffusion of the awareness. Granell *et al.*[28,29] studied the interaction between awareness diffusion and disease spreading on multiplex networks and revealed the existence of a critical value of the epidemic threshold, which is determined by the awareness and structure of the social layer. Benefitting from previous research, the interaction between resource allocation, awareness, and epidemic propagation has become a new research hotspot. The authors of Refs. 30 and 31 considered that awareness diffusion in virtual social networks cannot only change the daily behavior of individuals but also affect mutual assistance of resources among individuals. Resource support among friends during a pandemic is of prime importance to protect susceptible individuals from infection, especially when resources are severely scarce. Inspired by this, Wang *et al.*[32] studied the interplay between the processes of resource allocation, information diffusion and epidemic spreading on multiplex networks. Through theoretical analysis and simulation verification, they found that information diffusion and resource allocation cannot only affect the spread size of the epidemic, but also lead to distinct phase transitions underlying the epidemic outbreak. Moreover, the authors of Ref. 33 investigated the interaction between these three processes by adapting a metapopulation model. By considering the real social factors that can affect the coupled dynamics of the processes, they found that both information and geography can significantly impact the spread of the disease.

Despite extensive work on the interplay among resource allocation, information diffusion, and epidemic spreading, there are several scenarios that these studies have not considered. On one hand, because people in real life have limited energy and time to contact others,[34] they will interact selectively with each other during a small time interval, which will largely influence the spreading dynamics of the epidemic. Conversely, people acquire information about the epidemic from various channels, such as the global number of infected populations from social network platforms or mass media, and the number of infected neighbors from mouth to mouth in neighborhoods. Different types of information can induce different levels of concern in individuals. For example, the information about an infected neighbor has a more intuitive effect on an individual than the information on the global number of infected individuals acquired from television. Consequently, it is of interest and significance to understand how preferential contact among individuals and different types of information affect the coupled dynamics of awareness, resource allocation, and epidemic spreading.

To address these problems, an information-driven awareness-resource-epidemic model on top of multiplex networks is proposed in this study, which incorporates the elements of preferential contact and different types of information. We consider that the resources are allocated from healthy (susceptible) individuals to their infected

neighbors, and the allocation probability of each healthy individual is determined by its awareness that evolves dynamically with the immediate epidemic state. Information on the global infection density and the fraction of infected neighbors is considered in our model, which determines the awareness of each individual. To investigate the influence of different types of information on the coupled dynamics, two parameters that represent the relative weights of each piece of information are introduced in our model. For the transmission process of the disease, we consider that, owing to the limited energy and time of each individual, an infected individual contacts preferentially with a susceptible neighbor and transmits the disease to the selected neighbor with a certain probability. A parameter is introduced in our model to tune the preference. The recovery rate of each infected individual is determined by the number of resources received from neighbors in the social layer.

To theoretically analyze the coupled dynamics of the proposed model, we employ the Microscopic Markov Chain Approach (MMCA).[35] The infection density of the disease is predicted precisely, and an approximate epidemic threshold is derived using the evolution equations. Combining numerical analysis and experimental simulations, we systematically study the coupled dynamics from the following aspects: (1) We investigate the impact of information-driven awareness (which can affect the willingness of healthy individuals to allocate resources) on the dynamic characteristics of the coupled model, and find that the more active the resource support between individuals, the more effectively the disease can be controlled. (2) We further investigate the effects of preferential contact on the dynamical characteristics of the coupled model and find that there is a critical parameter at which the effectiveness of the disease control is the worst. Overall, the disease can be better suppressed when individuals with small degrees are preferentially protected. (3) Next, we study the effects of the inter-layer degree correlation and find that it has a "double-edged sword" effect on the coupled dynamics. Specifically, when there is a relatively lower infection rate, the more positive the inter-layer degree correlation, the better the disease can be suppressed. On the contrary, when there is a relatively larger infection rate, the more negative the inter-layer degree correlation, the more effectively the disease can be suppressed. (4) Finally, we study the relative weight of the two types of information, and find that the greater the weight of global information, the better the disease can be suppressed, which indicates that global information is of prime importance for disease control, and we need to increase information transparency during pandemic to optimally control the disease.

II. MODEL DESCRIPTIONS

In this section, an information-driven awareness-resource-epidemic model is proposed based on a double-layer multiplex network comprising social and physical contact layers. To distinguish the differences between the two layers, the social and contact layers are marked as A and B, respectively. We assume that resources are distributed among individuals with friend relationship on the social layer, which is consistent with most real social scenarios; namely, people are more inclined to help their friends when emergencies occur. It is assumed that the disease is transmitted from infected individuals to susceptible individuals in the physical contact layer.

The nodes and edges in the network represent individuals and their relationships.

A. Coupled dynamic model

In the contact layer of the network, a resource-based susceptible-infected-susceptible model is adapted to describe the spread of the epidemic. During each time interval $[t, t + \Delta t]$, the virus attempts to propagate from infected individuals to susceptible ones at a basic infection rate β. However, in real scenarios, an individual can interact with a limited number of people in a short period, and consequently, has to contact neighbors selectively.[36] To depict the preferential contact among nodes, a variable p_{ij} is introduced, such that in a time interval $(t, t + \Delta t)$, the probability of node i contacting j is p_{ij} which can be written as

$$p_{ij} = \frac{k_j^\chi}{\sum_{j \in \Omega_i^B} k_j^\chi}, \qquad (1)$$

where, Ω_i^B represents the neighbor set of node i in the contact layer, k_j is the degree of node j, and χ represents the contact preference located at $[-1.0, 1.0]$. When $\chi < 0$, individuals are more likely to contact neighbors with small degrees. When $\chi > 0$, individuals prefer to contact neighbors with large degrees. For $\chi = 0$, each individual randomly contacts a neighbor at a time. In addition, the infected nodes recover to the susceptible state at each time step. Because the recovery process of an infected node consumes a certain amount of resources, nodes with more resources will have a higher recovery probability. Consequently, the recovery rate of node i at time t is assumed to satisfy:

$$\mu_i(t) = 1 - (1 - \mu_0)^{\epsilon \omega_i(t) + 1}, \qquad (2)$$

where ϵ represents the resource conversion rate, which characterizes the extent to which the resources can improve the recovery rate,[21] $\omega_i(t)$ is the resources quantity of node i at time t, and μ_0 is the basic recovery rate of all nodes.

In addition, it is assumed that resources, such as drugs, protective supplies, and funds, are provided by healthy individuals.[32] In a small time interval, each susceptible node generates one unit of resource, and simultaneously allocates the resource to its infected neighbors. We consider that susceptible nodes can perceive the risk of contagion through information from both the mass media and the neighborhood in the social layer. Generally, individuals obtain information on the global number of infected individuals from mass media, simultaneously, they can acquire information about infected neighbors. These two types of information can have a distinct influence on the judgment of the risk of contagion for individuals. To investigate the impact of global and local information on spreading dynamics, we introduce the term *awareness*[27,28,37] denoted as α, to quantitatively characterize the perception of the contagion risk of susceptible individuals. To characterize the influence of the two types of information on the awareness of each individual, the global and local infected densities $\rho(t)$ and $\kappa(t)$ are used to represent the two types of information, which are calculated as follows:

$$\rho(t) = \frac{1}{N} \sum_{i=1}^{N} \rho_i(t), \qquad (3)$$

and

$$\kappa_i(t) = \frac{1}{k_i^A} \sum_{j \in \Omega_i^A} \rho_j(t), \tag{4}$$

where $\rho_i(t)$ is defined as the probability that node i is in the infected state at time t, $\kappa_i(t)$ is the fraction of infected neighbors of node i in the social layer at time t, Ω_i^A and k_i^A represent the neighbor set and the degree of node i in the social layer respectively. For simplicity, we denote $\rho \equiv \rho(t \to \infty)$ as the infection density in the steady state, and $\rho_i \equiv \rho_i(t \to \infty)$ as the infected probability of node i in the steady state. In addition, variables ζ and η are introduced to represent the relative weights of the global and local information respectively. According to the above definitions, the time dependent awareness of node i can be written as

$$\alpha_i(t) = 1 - (1 - \alpha_0)^{\zeta \rho(t) + \eta \kappa_i(t)}, \tag{5}$$

where the relationship between ζ and η satisfies $\zeta + \eta = 1$, and α_0 represents the basic awareness of the individuals. At each time step, the probability that a susceptible node allocates resources to its infected neighbor depends on its current awareness. A higher level of awareness implies lower willingness to allocate resources. Consequently, it is assumed that the relationship between the allocation probability of node i, denoted as $q_i(t)$, and the awareness $\alpha_i(t)$ satisfies:

$$q_i(t) = (1 - \alpha_i(t)). \tag{6}$$

Furthermore, it is assumed that the resources of each healthy node i are equally distributed to its infected neighbors with probability $q_i(t)$. Consequently, the resource quantity of each infected node j ($j = 1, \ldots, N$) at time t can be written as:

$$\omega_j(t) = \sum_{i \in \Omega_j^A} (1 - \rho_i(t)) \frac{q_i(t)}{\sum_{\ell \in \Omega_{i/j}^A} \rho_\ell(t) + 1}, \tag{7}$$

where $\Omega_{i/j}^A$ is the neighbor set of node i except j in the social layer.

B. Theoretical analysis of the model

In this section, MMCA is adapted to theoretically analyze the dynamic process of the model. According to the evolution rules described in the previous sections, the time evolution of $\rho_i(t)$ is:

$$\rho_i(t + \Delta t) = (1 - \rho_i(t))(1 - \pi_i(t)) + (1 - \mu_i(t)\Delta t)\rho_i(t), \tag{8}$$

where $\mu_i(t)\Delta t$ denotes the recovery probability of node i in the time interval $[t, t + \Delta t]$, and $\pi_i(t)$ is the probability that node i is not infected at time t. The first term on the right-hand side represents the probability that a susceptible node i is infected by one of its infected neighbors, and the second term is the probability that node i does not recover. The expression of $\pi_i(t)$ can be written as:

$$\pi_i(t) = \prod_{j \in \Omega_i^B} [1 - p_{ji} \beta \rho_j(t) \Delta t]. \tag{9}$$

In a small time interval, an individual has a limited opportunity to contact all its neighbors. Consequently, the probability that an infected node j contacts node i is p_{ji}. The probability that node i is infected by node j in the time interval $[t, t + \Delta t]$ is $p_{ji} \beta \rho_j(t) \Delta t$.

For convenience of analysis and without loss of generality, the time interval is set to $\Delta t = 1$, and Eqs. (8) and (9) can be rewritten as

$$\rho_i(t + 1) = (1 - \rho_i(t))(1 - \pi_i(t)) + (1 - \mu_i(t))\rho_i(t), \tag{10}$$

At a steady state, we have:

$$\rho_i = (1 - \rho_i)(1 - \pi_i) + (1 - \mu_i)\rho_i, \tag{11}$$

where π_i and μ_i are the probabilities of node i not being infected and the recovery rate of i in the steady state, respectively. By numerically iterating Eq. (11) for $i = 1, \ldots, N$, the infection probability of all nodes at each time step and the infection density ρ in the steady state can be obtained.

Because of the nonlinearities of the equations, we cannot obtain a theoretical expression for the epidemic threshold, which is a critical value in analyzing the spread of the epidemic. To derive the epidemic threshold β_c, we can resort to the approximate method. When $\beta \to \beta_c$, the infection probability of node i is $\rho_i \to 0$ for $i = 1, \ldots, N$. Thus, theoretical analysis can be performed by linearizing the equations in the vicinity of β_c. By applying the condition that $\rho_i \to 0$ for $i = 1, \ldots, N$ in the vicinity of β_c and incorporating Eq. (6) into Eq. (7), the approximation of the resource quantity of node i in the steady state ω_i can be expressed as:

$$\omega_i = \sum_{j \in \Omega_i^A} (1 - \alpha_j)$$

$$\approx \sum_{j \in \Omega_i^A} \left(\frac{\zeta}{N} + \frac{\eta}{k_j^A} \right) \alpha_0, \tag{12}$$

where α_i denotes the awareness of node i in the steady state. In addition, by linearizing Eqs. (2) and (11) and neglecting the high-order terms of the equations at a small value of μ_0, the following expression can be obtained:

$$\mu_i \approx \epsilon \omega_i \mu_0, \tag{13}$$

and

$$\rho_i = \frac{\beta}{\mu_i} \sum_{j=1}^{N} b_{ij} p_{ji} \rho_j \ \forall i = 1, \ldots, N, \tag{14}$$

where b_{ij} is an element of the adjacent matrix of the contact layer. By rewriting Eq. (14), we obtain the following iterative equation:

$$\rho_i(t + 1) = \frac{\beta}{\mu} [\mathbf{M} \boldsymbol{\rho}(t)]_i \ \forall i = 1, \ldots, N, \tag{15}$$

where the element of the matrix $\mathbf{M}$ is $M_{ij} = b_{ij} p_{ji}$ and $\boldsymbol{\rho}(t)$ is a column vector of the infected probability for all nodes. After a limited period, that is, $\Delta t = T$, the dynamic processes reach a stationary state, which satisfies the equation $\rho_i(t + 1) = \rho_i(t)$ for each time step t. Consequently, the following iterative equation is obtained:

$$\rho(T) = \beta D^{-1}(\boldsymbol{\mu}(T-1)) \mathbf{M} \boldsymbol{\rho}(T-1)$$

$$= \beta^T \left[\prod_{t=0}^{T-1} D^{-1}(\boldsymbol{\mu}(t)) \mathbf{M} \right] \boldsymbol{\rho}(0), \tag{16}$$

where the entries of the diagonal matrix $D(\boldsymbol{\mu}(t))$ are $D_{ii} = \mu_i(t)$ for $i = 1, 2 \cdots N$, and the matrix $D^{-1}(\mu(t))$ is the inverse of $D(\boldsymbol{\mu}(t))$.

Finally, the approximate expression of the epidemic threshold β_c can be derived based on the fact that when $\beta < \beta_c$, the epidemic gradually evolves to zero, that is, $\rho_i(t > T) \to 0$. Consequently, the following expression for β_c is obtained:

$$\beta_c = \left(\frac{1}{\Lambda_{\max} \left(\prod_{t=0}^{T-1} D^{-1}(\boldsymbol{\mu}(t)) \mathbf{M} \right)} \right)^{\frac{1}{T}}. \qquad (17)$$

The infection density ρ and threshold β_c are both influenced by preferential contact, inter-layer degree correlation, and individual awareness simultaneously.

III. NUMERICAL VERIFICATION AND SIMULATION RESULTS

In the following sections, we conduct both numerical analysis and extensive simulations to study the influence of information-driven awareness, contact preference and the structure of the underlying networks on the coupled dynamics on two-layer multiplex networks. In each simulation, a multiplex network of N nodes is built, and there is a one-to-one correspondence between the nodes in the two layers. Note that because simulations of the processes are extremely time-consuming, it is not feasible to perform all experiments on a network with a large number of nodes. In addition, the node quantity of the network has no qualitative influence on the relevant conclusions, as demonstrated in the Appendix section. Therefore, without loss of generality, the value of N is fixed at $N = 5000$ in this paper. The initial infection density is set to $\rho(0) = 0.1$ for all the simulation realizations. Because most network systems in the real world display the scale-free (SF) property,[38–41] we focus on SF-SF networks in numerical analysis and simulations.

In the simulations, the uncorrelated configuration model (UCM)[42] is applied to build both layers. The process of building the network is as follows.

i: Two degree sequences are generated according to the degree distributions $P(k) \sim k^{-\gamma_A}$ and $P(k) \sim k^{-\gamma_B}$, where γ_A and γ_B are the degree exponents of social and contact layers, respectively. Because the influence of the degree distribution on the coupled dynamics is not within the scope of this study and without loss of generality, the degree exponents of the two layers are fixed as $\gamma_A = \gamma_B = 2.4$ to avoid the influence of inconsistent degree distribution on the conclusions. The maximum degrees of the two layers are set to $k_{\max}^A = k_{\max}^B = \sqrt{N}$, which can avoid intra-layer degree correlation when the network size N is sufficiently large,[42,43] and to ensure that there are no isolated nodes in the generated network, the minimum degrees are restricted to $k_{\min}^A = k_{\min}^B = 3$.

ii: Each node in the two layers is randomly assigned a degree value. At each step, two nodes are randomly connected by an edge, and multiple edges and self-loops are prohibited. Subsequently, the degree values of the nodes at both ends of the edge decrease by one.

iii: Repeat step (ii) in the two layers simultaneously until the degree value of each node decreases to zero, and a multiplex network without inter and intra layer degree correlations is obtained.

The synchronous updating method[44] is adopted in the simulations. During a small time increment Δt, each infected node j attempts to infect its susceptible neighbor i with probability $p_{ji}\beta\Delta t$. Simultaneously, the infected node recovers to the susceptible state with probability $\mu_j(t)\Delta t$. Resource allocation occurs concurrently in the social layer. The coupled dynamics terminate when the global infected density fluctuates within a small range after a long time. To determine the epidemic threshold, we leverage the susceptibility measure Δ_χ[45] in the simulations, which is written as:

$$\Delta_\chi = N \frac{\langle \rho^2 \rangle - \langle \rho \rangle^2}{\langle \rho \rangle}, \qquad (18)$$

where $\langle \cdots \rangle$ is the ensemble average over all the realizations. The epidemic threshold β_c can be identified when the value of Δ_χ exhibits a diverging peak, which has been widely used in the identification of critical points in different scenarios.[45]

A. Effects of awareness and contact preference on the coupled dynamics

In this section, we investigate the influence of information-driven awareness on coupled dynamics using numerical analysis and extensive Monte Carlo simulations. To avoid the interference of other factors, we fix the coefficient of the inter-layer degree correlation π_d as 0 and the weight of global information at $\zeta = 0.5$. Figure 1 plots the infection density ρ as a function of the basic infection rate β for different values of α when the contact preference χ is $\chi = -1.0$ (a), 0 (b), and 1.0 (c). Initially, a fraction of $\rho(0) = 0.1$ nodes is randomly selected to be in the infected state, and the remaining nodes are in the susceptible state. The lines in the three subfigures represent the results obtained by the numerical iteration of Eq. (11) which matches well with the simulation results marked by the symbols. We can learn from Figs. 1(a) to 1(c) that, when χ is fixed, there is the largest value of the epidemic threshold β_c and the lowest value of ρ when $\alpha = 0.2$, and conversely, there is the smallest value of β_c and the largest value of ρ when $\alpha = 0.8$. The results obtained from the three subfigures indicate that, with the same contact preference, the more active the resource support between individuals, the more effectively the disease can be controlled.

To systematically study the impact of awareness on the coupled dynamics, we plot the full phase diagrams of the resource-epidemic coupled dynamics on the parameter plane $(\alpha - \beta)$ when the values of the contact preference are $\chi = -1.0$, $\chi = 0$ and $\chi = 1.0$ in Figs. 2(a)~2(c) respectively. The colors in the subfigures encode the infection density ρ in the stationary state. We can learn from the phase diagrams that at each fixed value of contact preference, the threshold β_c decreases monotonously with an increase in α. Specifically, when α approaches $\alpha = 1$, the value of β_c decreases sharply. Moreover, we find that when the infected nodes contact preferentially to neighbors with small degrees, for example, $\chi = -1.0$, the epidemic breaks out earlier and more sharply than when they prefer to contact neighbors with large degrees. When $\chi = 1.0$, as shown in Fig. 2(c), the threshold β_c increases significantly, and the increase of ρ slows distinctly with an increase in β. Preferential contact between the infected nodes and their neighbors has a significant influence on the coupled dynamics.
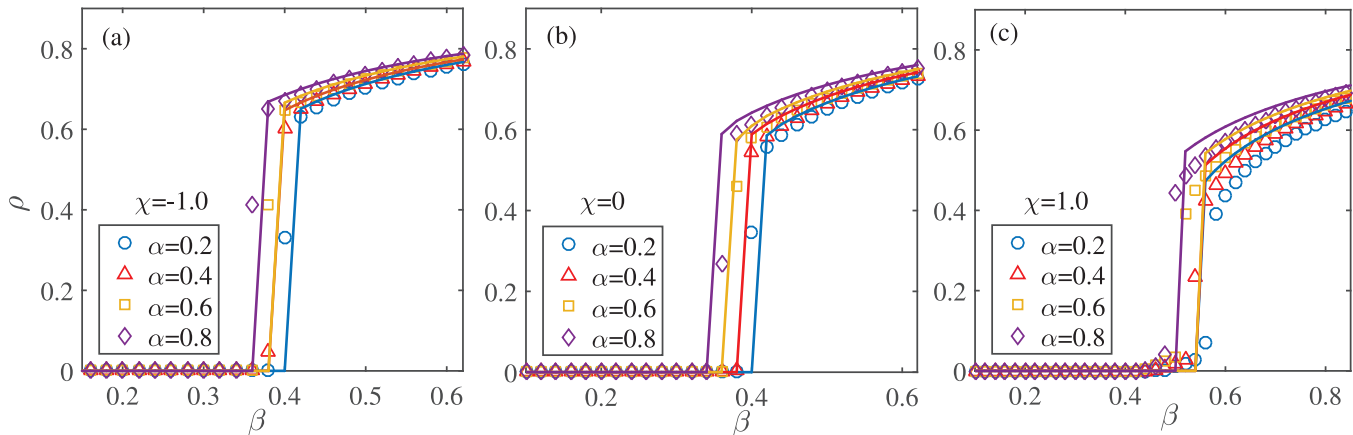
FIG. 1. Influence of the awareness on the coupled dynamics on double-layer networks without inter-layer degree correlation. The subfigures display the relationship between the values of ρ and β for $\alpha = 0.2$ (blue circles), $\alpha = 0.4$ (red triangles), $\alpha = 0.6$ (yellow squares) and $\alpha = 0.8$ (purple rhombuses) when $\chi = -1.0$ (a), $\chi = 0$ (b) and $\chi = 1.0$ (c), respectively. The other parameters are set to $\pi_d = 0$, $\zeta = 0.5$, the basic recovery rate is $\mu_0 = 0.1$. Lines in the subfigures represent the analytical results obtained from the MMCA. Data are obtained by averaging over 500 independent simulations.

To investigate the impact of preferential contact on the coupled dynamics, we first study the infection density ρ in the stationary state as a function of β for five typical values of χ when the basic awareness is fixed at $\alpha = 0.1$, 0.5 and 0.9, as shown in Figs. 3(a)~3(c). The symbols in the figures represent the simulation results, and the lines indicate the results obtained by MMCA. It can be observed from the figures that the theoretical results are in well agreement with the simulation results. In addition, it can be observed that overall, the more the infected nodes are inclined to contact neighbors with large degrees, the more the spread of the

disease can be suppressed. Specifically, it can be observed from the figures that when χ increases from $\chi = -1.0$ to $\chi = 1.0$, the spread size decreases and the threshold β_c increases. In addition, we find that, when $\chi \leq 0$, the spread size and threshold β_c are both close to each other for different levels of contact preference χ. However, when $\chi > 0$, the spread size decreases and the threshold β_c increases sharply with an increase in χ.

Furthermore, we systematically study the impact of preferential contact on the coupled dynamics by showing the epidemic threshold β_c as a function of χ when $\alpha = 0.1$, 0.5 and 0.9 in
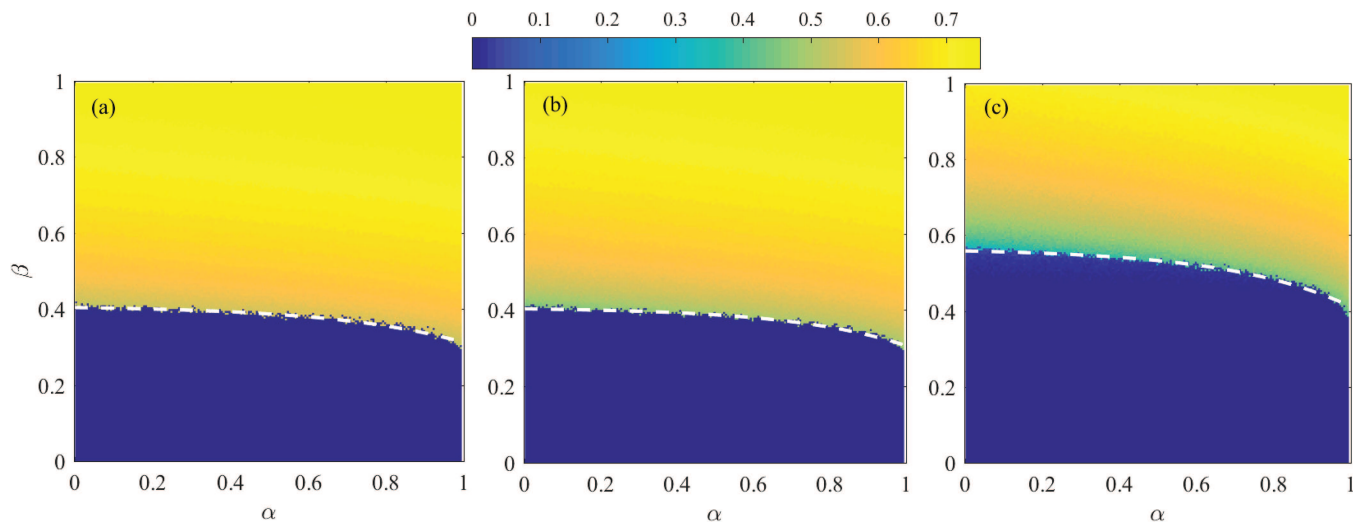
FIG. 2. The phase diagrams in the parameter plane $(\alpha - \beta)$ for $\chi = -1.0$ (a), $\chi = 0.0$ (b) and $\chi = 1.0$ (c) respectively. Colors in the subfigures represent the value of ρ obtained from Monte Carlo simulations. The white dotted lines indicate the theoretical predictions of epidemic threshold β_c obtained from Eq. (17).
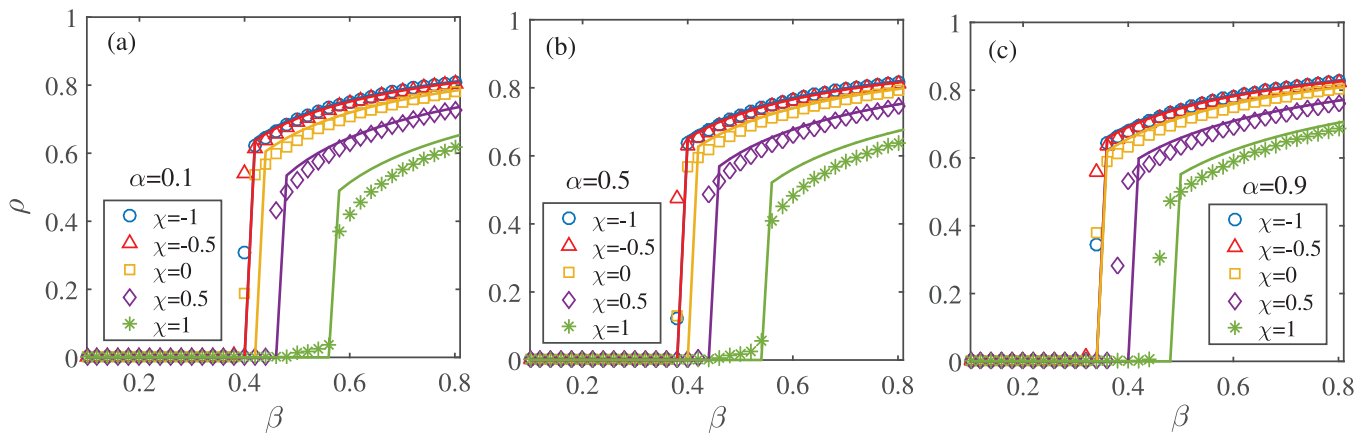
FIG. 3. Influence of the preferential contact on the coupled dynamics. The infection density ρ as a function of β when $\chi = -1$ (blue circles), -0.5 (red triangles), 0 (yellow squares), 0.5 (purple rhombuses) and 1 (green snowflakes) under the conditions that $\alpha = 0.1$ (a), $\alpha = 0.5$ (b) and $\alpha = 0.9$ (c). The other parameters are set to $\pi_d = 0$, $\zeta = 0.5$, $\mu_0 = 0.1$. Lines in the subfigures represent the analytical results obtained from the MMCA. Data are obtained by averaging over 500 independent Monte Carlo simulations.

Fig. 4. We can obtain the following conclusions from the figure. First, there is a critical value of χ denoted as χ^*; the epidemic threshold β_c decreases with χ when $\chi < \chi^*$, and conversely, it increases with χ when $\chi > \chi^*$. At point χ^*, the threshold β_c is the lowest and the spread size ρ is the largest. Second, at each fixed value of χ, the threshold decreases with increasing α, which is consistent with the results obtained in the previous section. Third, when $\chi > 0$ the disease can be better controlled than when $\chi < 0$.

B. Effects of inter-layer degree correlations on the coupled dynamics

In this section, we investigate the impact of inter-layer-degree correlations on the coupled dynamics. To build a double-layer multiplex network with inter-layer degree correlation π_d, we follow the following steps:

i: Two degree sequences are generated according to the degree distributions $P(k) \sim k^{-\gamma_A}$ and $P(k) \sim k^{-\gamma_B}$, where $\gamma_A = \gamma_B = 2.4$. The maximum and minimum degrees of the two layers are restricted to $k_{max}^A = k_{max}^B = \sqrt{N}$ and $k_{min}^A = k_{min}^B = 3$.

ii: Rematching both degree sequences in ascending order (maximum positive correlation) or rematching the degree sequence in the social layer in ascending order and the degree sequence in the contact layer in descending order (maximum negative correlation).

iii: Rematching any one of the sequences with probability $1 - \pi_d$.

iv: Assigning the degrees to each node according to the order or the degree sequences. Each pair of nodes is connected according to steps *ii* and *iii* in Sec. III A.

According to the above steps, we can obtained a double-layer multiplex network with a degree correlation π_d. In Figs. 5(a)~5(c), we show the infection density ρ as a function of β for different

inter-layer degree correlations when the awareness is $\alpha = 0.1$ (a), $\alpha = 0.5$ (b), and $\alpha = 0.9$ (c), respectively. In each subfigure, five typical values of π_d are chosen. From the figures, we find that for each fixed value of α, there is a critical point that is denoted as β^*. When $\beta < \beta^*$, the infection density ρ decreases monotonically with π_d, and the threshold β_c increases with π_d. This indicates that a positive inter-layer correlation is more conducive to delaying the epidemic outbreak. By contrast, when $\beta > \beta^*$, the infection density
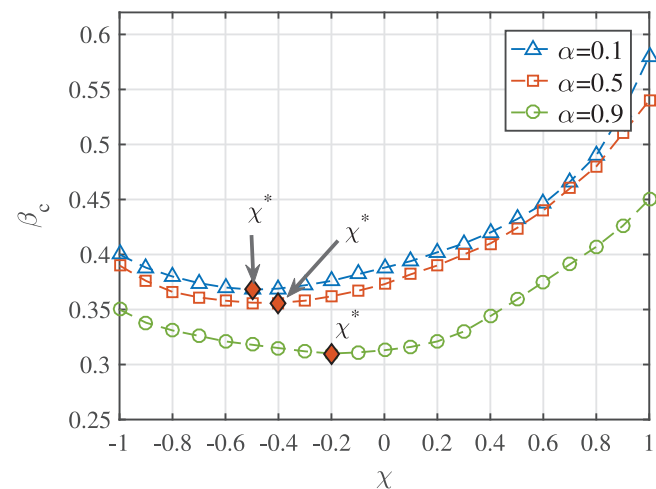
FIG. 4. The epidemic threshold β_c as a function of χ for $\alpha = 0.1$ (red squares), $\alpha = 0.5$ (green circles) and $\alpha = 0.9$ (blue triangles). The red rhombuses represent the critical value χ^*, at which β_c reaches to the lowest value. The other parameters are set to $\pi_d = 0$, $\zeta = 0.5$, $\mu_0 = 0.1$ respectively.
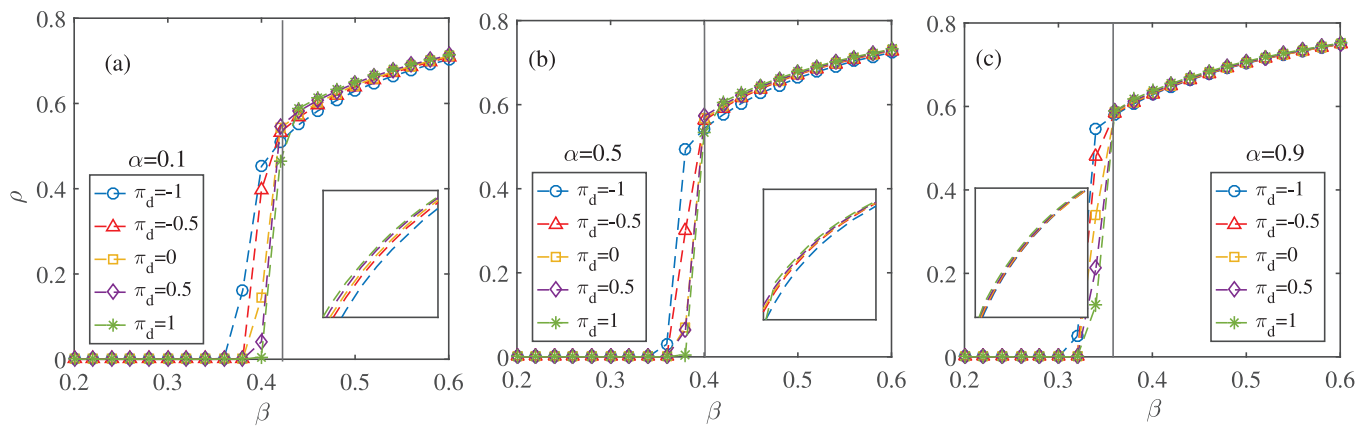
FIG. 5. Impacts of inter-layer degree correlation on the coupled dynamics. The infection density ρ at the steady state as a function of β when $\pi_d = -1$ (blue circles), -0.5 (red triangles), 0 (yellow squares), 0.5 (purple rhombuses) and 1 (green snowflakes) under the conditions that $\alpha = 0.1$ (a), $\alpha = 0.5$ (b) and $\alpha = 0.9$ (c). The inset in each subfigure is the the partial enlarged details of the curves after the cross point. The other parameters are set to $\chi = 0$, $\zeta = 0.5$, $\mu_0 = 0.1$. Data are obtained by averaging over 500 independent Monte Carlo simulations.

ρ increases with π_d. This result suggests that when there is a relatively high infection rate, a negative inter-layer correlation will be more conducive to the suppression of disease transmission.

We can qualitatively explain the phenomena above as follows. Previous studies have demonstrated that the propagation process of the epidemic exhibits hierarchical features in networks.[46] Namely, in the initial stage of propagation, the disease is located on a small finite number of nodes in the contact layer, where the hub nodes with large degrees are the centers of localization,[47] and then, slowly propagates to other nodes through edges linked

to these hub nodes when there is a relatively smaller infection rate, that is, $\beta < \beta^*$. Consequently, when there is a positive inter-layer degree correlation, an infected hub node has a high probability of obtaining adequate resources from its neighbors in the social layer, which ensures a high recovery rate for the infected nodes. A large recovery rate of the entire system can then lower the effective infection rate of the disease, which can be defined as $\beta_e = \beta/\langle\mu\rangle$, where $\langle\mu\rangle$ is the average recovery rate of all nodes[21,48]. Conversely, when there is a relatively larger infection rate, that is, $\beta > \beta^*$, the disease propagates rapidly to a large proportion
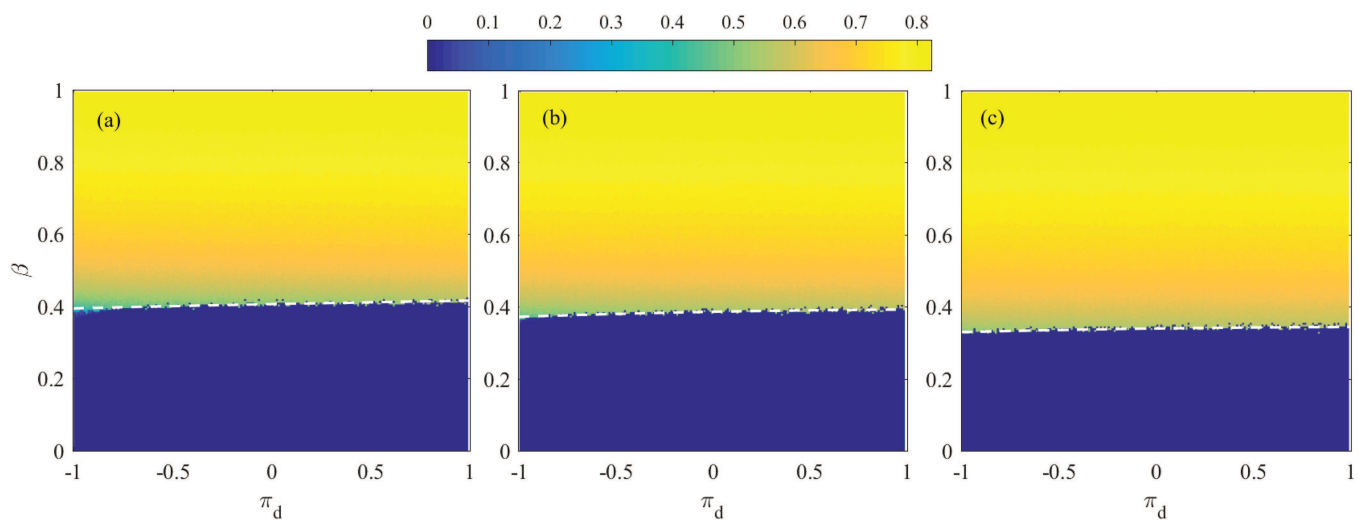
FIG. 6. The phase diagrams in the parameter plane $(\pi_d - \beta)$ for $\alpha = 0.1$ (a), $\alpha = 0.5$ (b) and $\alpha = 0.9$ (c). Colors in the figures represent the value of ρ obtained from Monte Carlo simulations. The white dotted lines indicate the theoretical predictions of epidemic threshold β_c obtained from MMCA.
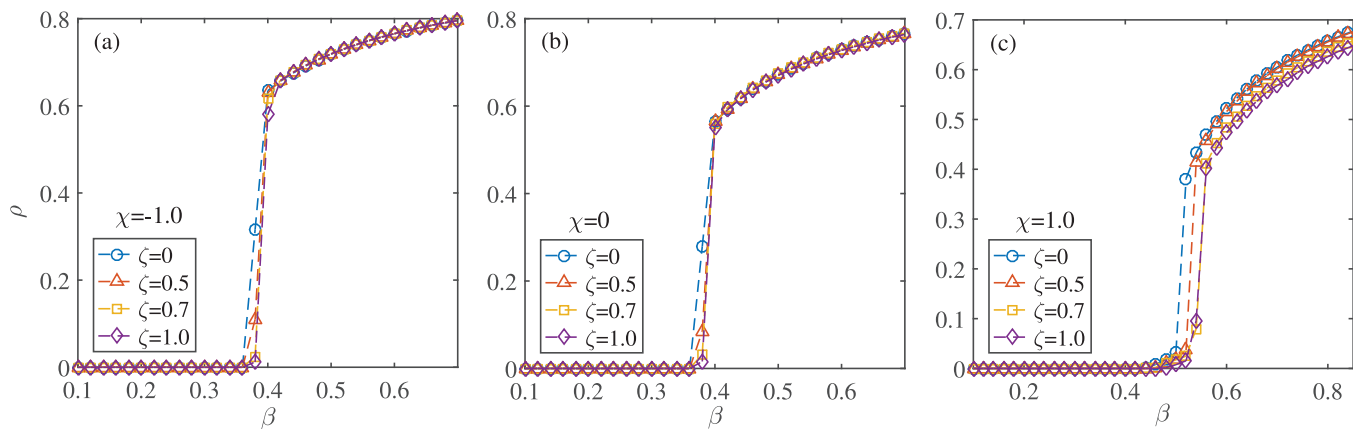
FIG. 7. Influence of global and local information on the coupled dynamics. (a) Infected density ρ as a function of β for $\zeta = 0$ (blue circles), 0.5 (red triangles), 0.7 (yellow squares) and 1.0 (purple rhombuses) when contact preference is $\chi = -1.0$. Subfigures (b) and (c) are the cases when $\chi = 0$ and $\chi = 1.0$ respectively. The other parameters are set to $\pi_d = 0$ and $\alpha = 0.5$, $\mu_0 = 0.1$. Data are obtained by averaging over 500 independent Monte Carlo simulations.

of the network. Under this condition, a more negative inter-layer correlation indicates that the nodes with small degrees in the contact layer will have a larger probability of having a counterpart with large degrees in the social layer, and then, a higher probability of obtaining more resources and a higher recovery rate for most of the nodes in the contact layer. Scale-free networks comprise a large proportion of nodes with small degrees and a small proportion of nodes with large degrees. Consequently, when $\beta > \beta^*$, a more negative inter-layer degree correlation is beneficial for suppressing the spread of the epidemic.

Further, we study systematacially the influence of the inter-layer degree correlation on the results by presenting the full phase diagrams in parameter $(\pi_d - \beta)$ for $\alpha = 0.1$ (a), $\alpha = 0.5$ (b), and $\alpha = 0.9$ (c) in Fig. 6 respectively. Colors in the subfigures encode the infection density ρ, and the white lines indicates the threshold β_c as a function of π_d that is obtained from MMCA. We find that, overall, the epidemic threshold β_c increases monotonously with the increase of π_d when the value of π_d changes from -1.0 to 1.0. In addition, we can also find that the difference of β_c for different inter-layer degree correlation is smaller at a larger awareness, i.e., $\alpha = 0.9$, than that of a smaller awareness, i.e., $\alpha = 0.1$.

C. Effects of global and local information on the coupled dynamics

Finally, we focus on the impact of global and local information on coupled dynamics. Individuals can perceive the risk of contagion through information disseminated from mass media, such as social platforms, TV news, and newspapers, and the infection of their friends,[49] which can then change the awareness of people.[50] Subsequently, they react heterogeneously to the information, such as maintaining social distancing and stockpiling supplies.[4] In turn, the change in awareness and behaviors of people will affect the coupled dynamics of resource allocation and disease spread.

To study influence of the global and local information on the coupled dynamics, we exhibit the infection rate ρ as a function of β for four typical weights of global information in Fig. 7, namely, $\zeta = 0$ (blue circles), $\zeta = 0.5$ (red triangles), $\zeta = 0.7$ (yellow squares) and $\zeta = 1.0$ (purple rhombuses), the results for the other values of ζ are exhibited in the Appendix section. The relative weight of local information can be obtained by $\eta = 1 - \zeta$. We find that when the infected nodes contact randomly, i.e., $\chi = 0$, or preferentially to the neighbors with small degrees $\chi = -1.0$, the relative weights of the global and local information do not affect the infection density ρ and epidemic threshold β_c. In contrast, when nodes with large degrees are contacted preferentially, the epidemic threshold β_c does not change, whereas the value of ρ decreases with an increase in the relative weight of global information ζ.

IV. CONCLUSIONS AND DISCUSSIONS

In this study, we examined the interaction among information-driven awareness, resource allocation, and epidemic spreading on top of multiplex networks from more realistic perspectives. A multiple coupled model that incorporates the factors of the preferred contact among individuals, different types of information and the inter-layer degree correlation, has been proposed. We have considered that in the real scenario, awareness, resource allocation and epidemic spreading interact with each other through the following mechanism: the rapid spread of the disease stimulates the diffusion of information about the disease, and susceptible individuals perceive the risk of contagion from both global and local information, which alters the behavior of the individuals. Susceptible individuals can provide resources to assist the recovery of infected neighbors, which is affected by their information-driven awareness. Subsequently, the recovery rate of the infected individuals is dependent on the resources received from susceptible neighbors, which in turn influences the spreading dynamics of the epidemic. To distinguish between the two types of information,

the parameters ζ and η were introduced in the model to represent the relative weights of global and local information respectively. In addition, we introduced the parameter χ to tune the contact preferences, such that, when $\chi < 0$, the infected nodes in the contact layer are more likely to contact susceptible neighbors with small degrees; otherwise, they are more likely to contact those with large degrees.

To analyze the coupled dynamics theoretically, we employed the MMCA theory. The infection density was precisely predicted using MMCA. Moreover, we obtained an approximate epidemic threshold using this theory. By using both theoretical analysis and Monte Carlo simulations on multiplex networks, we conducted our research from the following four aspects: (1) We studied the impact of awareness on the coupled dynamics and found that with the increase in α, the infection density in the stationary state increases and the epidemic threshold β_c decreases monotonously. The results suggest that during a pandemic, the more active the resource support between individuals, the more effectively the disease can be controlled. (2) Further, we investigated the impact of preferential contact on the coupled dynamics, and found that when the parameter χ increases from -1.0 to 1.0, the threshold β_c first decreases until it reaches a critical value χ^*, and then increases with χ. At $\chi = \chi^*$, the value of β_c is the lowest and the infection density ρ is the highest. Moreover, there is a maximum value of β_c at $\chi = 1.0$, which indicates that it is more conducive to suppressing the disease when the nodes with small degrees are better protected. (3) Next, we studied the impact of the inter-layer degree correlation on the results, and found that the inter-layer degree correlation has a "double-edged sword" effect on the spreading dynamics. Specifically, there is a critical value β^*. When $\beta < \beta^*$, the outbreak of the disease can be delayed with an increase in the value of π_d. On the contrary, when $\beta > \beta^*$, the infection density ρ increases with π_d. (4) Finally, we studied the impact of different types of information on the coupled dynamics, and found that when the infected nodes preferentially contact the neighbors with small degrees, the information type has little impact on the results, while, when they contact preferentially the neighbors with large degrees, the infection density ρ decreases with an increase in the relative weight of global information ζ, which suggests that global information is more effective in suppressing the disease.

Our findings make a strong contribution to the understanding of the mechanisms by which information-driven awareness, the behavior of resource allocation, and the spread of the epidemic interact in more real scenarios. The results of this study are of practical significance for controlling outbreaks of infectious diseases. It will also guide us to behave reasonably when perceiving the threat of disease. Based on the conclusions of this study, we propose possible suggestions for epidemic control. First, in the early stages of an epidemic, people should maintain rational attitudes and behaviors to avoid "panic buying" and hoarding resources.[51] They should be encouraged to support and help each other by donating resources more actively to suppress or mitigate the spread of an epidemic. Second, during a pandemic, governments should increase information transparency of the disease by increasing the dissemination of information about the state of the epidemic through public channels.

AUTHOR DECLARATIONS

Conflict of Interest

The authors have no conflicts to disclose.

Author Contributions

Jun Wang: Data curation (equal); Investigation (equal); Validation (equal); Visualization (lead); Writing – original draft (lead); Writing – review and editing (equal). **Weijie Xiong:** Investigation (equal); Validation (equal); Visualization (equal); Writing – original draft (equal). **Ruijie Wang:** Conceptualization (lead); Formal analysis (lead); Funding acquisition (lead); Investigation (equal); Methodology (lead); Supervision (lead); Validation (lead); Writing – original draft (equal); Writing – review and editing (lead). **Shimin Cai:** Funding acquisition (equal); Investigation (equal); Methodology (equal). **Die Wu:** Funding acquisition (equal); Investigation (equal); Methodology (equal); Writing – original draft (equal). **Wei Wang:** Formal analysis (equal); Funding acquisition (equal); Validation (equal); Writing – review and editing (equal). **Xiaolong Chen:** Conceptualization (equal); Funding acquisition (equal); Investigation (equal); Methodology (equal); Supervision (equal); Writing – review and editing (equal).

DATA AVAILABILITY

The data supporting the findings of this study are available from the corresponding author upon reasonable request.

APPENDIX

In this section, we first show the results of the supplementary experiments for the influence of global and local information on coupled dynamics. Different from Fig. 7, we choose two relatively small values of the weight of global information ζ in Fig. 8, namely $\zeta = 0.1$ (blue circles), $\zeta = 0.3$ (red triangles). For comparison, the results of $\zeta = 0.5$ (green squares) are also exhibited in the three subfigures. We find that when $\zeta = 0.1$ and $\zeta = 0.3$, the conclusions are exactly the same as those in Fig. 7.

To explore the impact of network size on the results and confirm that it does not qualitatively affect the results, we conduct supplementary simulations on networks with size $N = 10^6$. Note that when the network size is relatively large, i.e., $N = 10^6$, the corresponding calculations are extremely time-consuming; therefore, it is not feasible to reproduce all the experiments on these networks. Consequently, we exhibit two typical results, as shown in
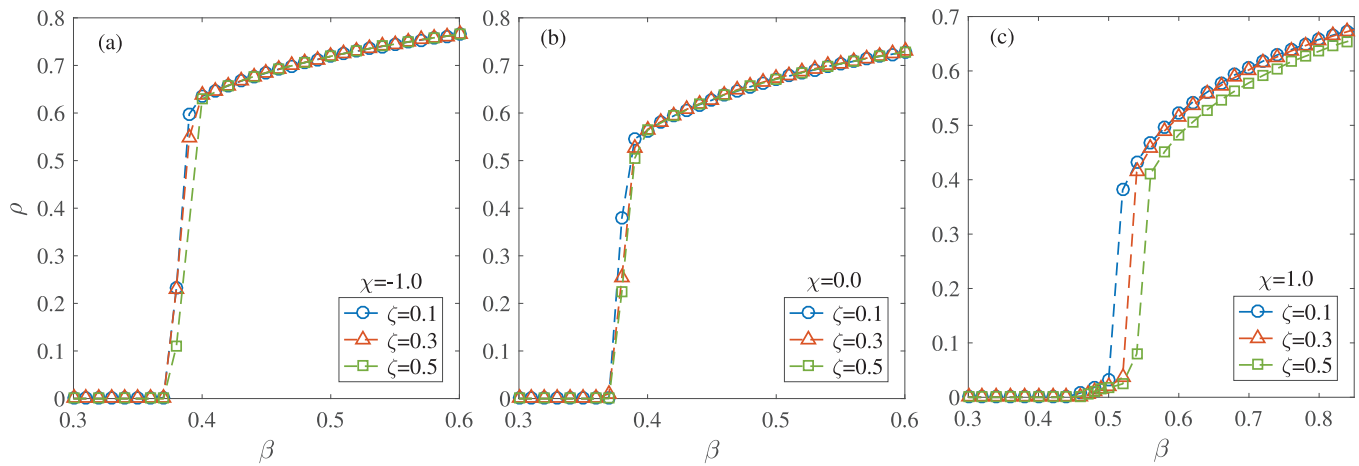
FIG. 8. Supplementary figures of the experiments for the influence of global and local information on the coupled dynamics. The values of the relative weight of global information are set to $\zeta = 0.1$, $\zeta = 0.3$ and $\zeta = 0.5$ for $\chi = -1.0$ (a), $\chi = 0$ (b) and $\chi = 1.0$ (c) respectively. The other parameters are exactly the same as those in Fig. 7.

Figs. 9 and 10. In Fig. 9, we show the results of the infection density ρ in the steady state as a function of β for four values of α when $\chi = 0$, which corresponds to the results in Fig. 1(b). In Fig. 10, we show the results for ρ as a function of β for five values of χ when $\alpha = 0.5$, which corresponds to the results in Fig. 3(b). Note that the other parameters of the two figures are the same as those of the corresponding figures.

corresponding figures. It can be observed in Figs. 9 and 10 that, the corresponding conclusions remain unchanged. There is only a small range of changes in the absolute values of the epidemic threshold β_c and the infection density ρ. Consequently, without affecting the conclusions, a relatively small network size, $N = 5000$ was selected in the main text to reduce the calculation time.
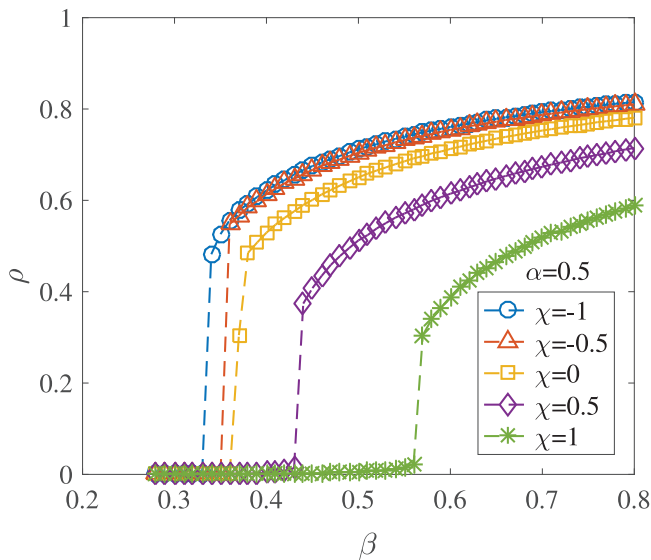
FIG. 9. Illustration of the simulation results on network with node size $N = 10^6$ corresponding to Fig. 1(b)
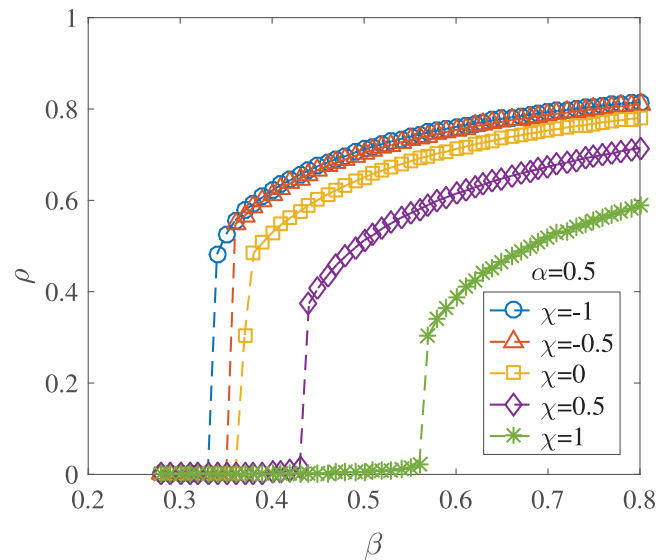
FIG. 10. Illustration of the simulation results on network with node size $N = 10^6$ corresponding to Fig. 3(b)

REFERENCES

[1] L. O. Gostin and E. A. Friedman, The Lancet **385**, 1902 (2015).

[2] D. E. McMahon, G. A. Peters, L. C. Ivers, and E. E. Freeman, PLoS Neglected Trop. Dis. **14**, e0008412 (2020).

[3] Geneva: Organization, "WHO covid-19 dashboard," https://covid19.who.int/ (2020).

[4] W. Xie, S. Campbell, and W. Zhang, Proc. Natl. Acad. Sci. **117**, 17667 (2020).

[5] M. M. Queiroz, D. Ivanov, A. Dolgui, and S. F. Wamba, Annals of Operations Research **2020**, 1.

[6] W. McKibbin and R. Fernando, Asian Economic Papers **20**, 1 (2021).

[7] A. Spinelli and G. Pellino, Journal of British Surgery **107**, 785 (2020).

[8] M. L. Ranney, V. Griffeth, and A. K. Jha, N. Engl. J. Med. **382**, e41 (2020).

[9] R. M. Anderson, H. Heesterbeek, D. Klinkenberg, and T. D. Hollingsworth, The Lancet **395**, 931 (2020).

[10] J. Bedford, D. Enria, J. Giesecke, D. L. Heymann, C. Ihekweazu, G. Kobinger, H. C. Lane, Z. Memish, M.-D. Oh, A. Schuchat et al., The Lancet **395**, 1015 (2020).

[11] C. Nowzari, V. M. Preciado, and G. J. Pappas, IEEE Transactions on Control of Network Systems **4**, 159 (2015).

[12] N. J. Watkins, C. Nowzari, V. M. Preciado, and G. J. Pappas, IEEE Transactions on Control of Network Systems **5**, 298 (2016).

[13] V. M. Preciado, F. D. Sahneh, and C. Scoglio, in 2013 IEEE Global Conference on Signal and Information Processing (IEEE, 2013), pp. 851–854.

[14] V. M. Preciado, M. Zargham, C. Enyioha, A. Jadbabaie, and G. J. Pappas, IEEE Transactions on Control of Network Systems **1**, 99 (2014).

[15] H. Chen, G. Li, H. Zhang, and Z. Hou, Phys. Rev. E **96**, 012321 (2017).

[16] A. Y. Lokhov and D. Saad, Proc. Natl. Acad. Sci. **114**, E8138 (2017).

[17] L. Pan, W. Wang, L. Tian, and Y.-C. Lai, Phys. Rev. E **103**, 012302 (2021).

[18] C. J. Worby and H.-H. Chang, Nat. Commun. **11**, 1 (2020).

[19] Z. Wang, M. A. Andrews, Z.-X. Wu, L. Wang, and C. T. Bauch, Physics of Life Reviews **15**, 1 (2015).

[20] J. S. Weitz, S. W. Park, C. Eksin, and J. Dushoff, Proc. Natl. Acad. Sci. **117**, 32764 (2020).

[21] X. Chen, R. Wang, D. Yang, J. Xian, and Q. Li, Complexity **2020**, 8861493, (2020).

[22] W. Li, X. Xue, L. Pan, T. Lin, and W. Wang, Applied Mathematics and Computation **412**, 126595 (2022).

[23] L. He and L. Zhu, Commun. Theor. Phys. **73**, 035002 (2021).

[24] S. S. Musa, S. Qureshi, S. Zhao, A. Yusuf, U. T. Mustapha, and D. He, Infectious Disease Modelling **6**, 448 (2021).

[25] Z. Wang, M. Jusup, H. Guo, L. Shi, S. Geček, M. Anand, M. Perc, C. T. Bauch, J. Kurths, S. Boccaletti, H. J. Schellnhuber, Proc. Natl. Acad. Sci. **117**, 17650 (2020).

[26] P. Huang, X.-L. Chen, M. Tang, and S.-M. Cai, Complexity **2021**, 6629105, (2021).

[27] S. Funk, E. Gilad, C. Watkins, and V. A. Jansen, Proc. Natl. Acad. Sci. **106**, 6872 (2009).

[28] C. Granell, S. Gómez, and A. Arenas, Phys. Rev. Lett. **111**, 128701 (2013).

[29] C. Granell, S. Gómez, and A. Arenas, Phys. Rev. E **90**, 012808 (2014).

[30] X. Chen, Q. Liu, R. Wang, Q. Li, and W. Wang, Complexity **2020**, 3256415, (2020).

[31] X. Chen, K. Gong, R. Wang, S. Cai, and W. Wang, Applied Mathematics and Computation **385**, 125428 (2020).

[32] X. Wang, X. Zhu, X. Tao, J. Xiao, W. Wang, and Y.-C. Lai, Phys. Rev. Res. **3**, 013157 (2021).

[33] X. Zhu, Y. Liu, S. Wang, R. Wang, X. Chen, and W. Wang, Applied Mathematics and Computation **411**, 126531 (2021).

[34] R. Yang, L. Huang, and Y.-C. Lai, Phys. Rev. E **78**, 026111 (2008).

[35] S. Gómez, A. Arenas, J. Borge-Holthoefer, S. Meloni, and Y. Moreno, EPL (Europhysics Letters) **89**, 38009 (2010).

[36] R. Yang, T. Zhou, Y.-B. Xie, Y.-C. Lai, and B.-H. Wang, Phys. Rev. E **78**, 066109 (2008).

[37] K. A. Kabir, K. Kuga, and J. Tanimoto, Chaos, Solitons Fractals **132**, 109548 (2020).

[38] M. Girvan and M. E. Newman, Proc. Natl. Acad. Sci. **99**, 7821 (2002).

[39] Z. Liu, Y.-C. Lai, and N. Ye, Phys. Rev. E **67**, 031911 (2003).

[40] M. Small, Y. Li, T. Stemler, and K. Judd, Phys. Rev. E **91**, 042801 (2015).

[41] Z. Wang, C. Wang, X. Li, C. Gao, X. Li, and J. Zhu, IEEE Transactions on Knowledge and Data Engineering **34**, 1206 (2020).

[42] M. Catanzaro, M. Boguñá, and R. Pastor-Satorras, Phys. Rev. E **71**, 027103 (2005).

[43] M. Boguñá, R. Pastor-Satorras, and A. Vespignani, The European Physical Journal B-Condensed Matter and Complex Systems **38**, 205 (2004).

[44] B. Schönfisch and A. de Roos, BioSystems **51**, 123 (1999).

[45] S. C. Ferreira, C. Castellano, and R. Pastor-Satorras, Phys. Rev. E **86**, 041125 (2012).

[46] M. Barthélemy, A. Barrat, R. Pastor-Satorras, and A. Vespignani, Phys. Rev. Lett. **92**, 178701 (2004).

[47] A. V. Goltsev, S. N. Dorogovtsev, J. G. Oliveira, and J. F. Mendes, Phys. Rev. Lett. **109**, 128702 (2012).

[48] R. Pastor-Satorras, C. Castellano, P. Van Mieghem, and A. Vespignani, Rev. Mod. Phys. **87**, 925 (2015).

[49] B. Vai, S. Cazzetta, D. Ghiglino, L. Parenti, G. Saibene, M. Toti, C. Verga, A. Wykowska, and F. Benedetti, Frontiers in Psychology **11**, 563426 (2020).

[50] J. J. Van Bavel, K. Baicker, P. S. Boggio, V. Capraro, A. Cichocka, M. Cikara, M. J. Crockett, A. J. Crum, K. M. Douglas, J. N. Druckman et al., Nature Human Behaviour **4**, 460 (2020).

[51] J. J. V. Bavel, K. Baicker, P. S. Boggio, V. Capraro, A. Cichocka, M. Cikara, M. J. Crockett, A. J. Crum, K. M. Douglas, J. N. Druckman et al., Nature Human Behaviour **4**, 460 (2020).